Biochemical Pharmacology 80 (2010) 39–49

Contents lists available at ScienceDirect

Biochemical Pharmacology

journal homepage: www.elsevier.com/locate/biochempharm

Inhibition of epidermal growth factor receptor-overexpressing cancer cells by camptothecin, 20-(N,N-diethyl) glycinate

V. Badireenath Konkimalla, Thomas Efferth *

German Cancer Research Center, Pharmaceutical Biology (C015), Heidelberg, Germany

ARTICLE INFO

Article history:
Received 8 December 2009
Accepted 25 February 2010

Keywords:
Chemotherapy
Microarray
Oncogenes
Pharmacology
Pharmacogenomics
Signal transduction
Systems biology

ABSTRACT

The epidermal growth factor receptor (EGFR) represents a prognostic marker for short survival of patients and therapy resistance of tumors. Despite clinical usefulness of EGFR tyrosine kinase inhibitors, resistance can develop. Therefore, there is an urgent need for novel EGFR inhibitors. Camptothecins have been characterized as inhibitors of DNA topoisomerase I (TOP1), although a correlation between TOP1 expression and activity is not well established in clinical biopsies. Hence, other targets may also be relevant. By molecular docking, we found that camptothecin 20-N,N-glycinate (CPTg) and camptothecin (CPT) bind to the same pharmacophore at EGFR as erlotinib, albeit to partly different amino acids. To validate the *in silico* results, CPT and CPTg were evaluated for their cytotoxic activity and downstream signaling mechanisms in U87MG glioblastoma cell lines transduced with different expression vectors for *EGFR*. All transduced cell lines were more susceptible to CPTg or CPT than the non-transduced cells, indicating a preferential activity towards EGFR-expressing tumor cells. Microarray-based mRNA hybridizations were performed in treated a non-treated cell lines. Subsets of genes were commonly regulated between the cell lines. By pathway analyses, we ranked canonical pathways according to differential gene expression after drug treatment. The pathways for G2/M DNA damage checkpoint regulation, aryl hydrocarbon receptor signaling, and xenobiotic metabolism and endoplasmatic reticulum stress were top ranked. In conclusion, binding of CPTg and CPT to the erlotinib pharmacophore and preferential cytotoxicity towards EGFR-overexpressing cells indicate susceptibility towards erlotinib-resistant tumors. Multiple mechanisms may account for cytotoxicity of these camptothecins.
© 2010 Elsevier Inc. All rights reserved.

1. Introduction

The epidermal growth factor receptor (EGFR) gene family is of eminent importance as prognostic marker in cancer patients [1–5]. Four members have been identified in humans (*HER1–HER4*), of which HER1 (EGFR, *erbB1*) and HER2 (*erbB2*, *c-neu*) are best characterized. They are glycoproteins, which bind EGFR and other ligands and activate downstream signaling routes involved in cancer biology. HER1 and HER2 are frequently overexpressed in tumors and are associated with short survival times of patients and therapy resistance of tumors.

EGFR molecules are inactive monomers that are activated by homodimerization with a second EGFR molecule or with another HER member (i.e., HER2). The dimerization stimulates the intrinsic tyrosine kinase activity of EGFR, which regulates specific signal transduction cascades. Constitutive EGFR activation as a consequence of mutations or gene amplification causes deregulated cellular processes, such as proliferation, invasion, angiogenesis, cell motility, cell adhesion, inhibition of apoptosis, and DNA synthesis. The kinase activity is also associated with autophosphorylation of five tyrosine residues in the C-terminal EGFR domain. Specific EGFR mutations foster the development of tumors [6].

The extraordinary relevance of EGFR in tumor biology makes it an exquisite target for cancer therapy. Apart from therapeutic antibodies, several small molecules have been developed as EGFR inhibitors [7]. For example, gefitinib (Iressa®, Astra Zeneca, DE, USA) and erlotinib (Tarceva®, Genentech Inc., CA, USA) are used for the treatment of non-small cell lung cancer and other tumor types [8]. Both compounds belong to the class of quinazolinamines and exhibit their inhibitory activity on EGFR tyrosine kinases by competing with ATP for the ATP-binding pocket.

Despite the clinical usefulness of EGFR tyrosine kinase inhibitors, resistance can develop by selection of point-mutated EGFR variants [9]. Therefore, there is an urgent need for the identification of novel EGFR tyrosine kinase inhibitors for treating tumors carrying such EGFR mutants.

Camptothecin is a natural product derived from the Chinese tree, *Camptotheca accuminata*. Its derivatives, irinotecan and

* Corresponding author at: Department of Pharmaceutical Biology, Institute of Pharmacy and Biochemistry, University of Mainz, Staudinger Weg 5, 55128 Mainz, Germany. Tel.: +49 6131 39 25751; fax: +49 6131 39 23752.
E-mail address: efferth@uni-mainz.de (T. Efferth).

0006-2952/$ – see front matter © 2010 Elsevier Inc. All rights reserved.
doi:10.1016/j.bcp.2010.02.022

topotecan, belong to the most successful anti-cancer drugs in the armory to treat cancer. They are used to treat gynecological tumors, metastasized colorectal carcinomas, advanced non-small cell lung cancer. Camptothecins have been characterized as inhibitors of DNA topoisomerase I. This enzyme induces DNA single strand breaks allowing DNA relaxation for replication. The breakage and closure reactions generated by DNA topoisomerase I are reversible. Camptothecin analogues, including topotecan and irinotecan, inhibit the closure reaction of the enzyme thereby leading to cell death of tumor cells [10].

Despite the clinical success of camptothecins, a correlation between DNA topoisomerase I activity or expression is not well established in cell lines and clinical biopsies [11–13]. This indicates that camptothecins may not only act by inhibiting DNA topoisomerase I, but that other targets may also be relevant for the activity of this drug class in cancer cells.

Interestingly, several correlation studies found significant associations between the activity of camptothecins and the epidermal growth factor receptor expression implying a possible role of EGFR for sensitivity and resistance to this drug class [14,15].

Recently, we set up a database with phytochemicals from medicinal plants used in traditional Chinese medicine [16,17]. We exploited this database by a virtual screening approach using three-dimensional modeling to find novel inhibitors of the epidermal growth factor receptor. Interestingly, we identified a camptothecin derivative, camptothecin, 20-(N,N-diethyl) glycinate (NSC 364830), which bound *in silico* with high affinity to the tyrosine kinase domain of EGFR. This indicates that this derivative might be an inhibitor of EGFR contributing to the cytotoxic activity of this compound towards cancer cells.

The aim of the present investigation was to analyze this hypothesis in more detail. For this reason, we used U87MG human glioblastoma wild-type cells and sublines thereof either transduced with expression vectors harboring cDNAs for deletion-activated EGFR (U87MG.ΔEGFR), point-mutated EGFR (U87MG.DK2-N), or wild-type EGFR (U87MG.wtEGFR). These cell lines were treated with camptothecin, 20-(N,N-diethyl) glycinate as well as with the lead drug, camptothecin. To get insight into the molecular signaling routes that may be associated with the activity of camptothecin, 20-(N,N-diethyl) glycinate and camptothecin in EGFR-transduced glioblastoma cell lines, microarray-based transcriptome-wide mRNA expression profiling and pathway profiling analyses were performed.

2. Materials and methods

2.1. Three-dimensional docking

The crystal structure of EGFR tyrosine kinase domain (EGFR-TK) bound to erlotinib (PDB1M17) served as the receptor template. Erlotinib was used as a clinically established positive control, because it specifically binds to EGFR-TK and inhibits signal transduction of EGFR. To carry out the docking operation of unbound EGFR-TK with our test compounds, erlotinib has *in silico* been removed from the EGFR-TK–erlotinib crystal structure. Essential hydrogens were added and the protein was solvated with water as solvent. A grid of 60 $Å^3$, 0.375 Å spacing was first computed in order to sample the binding site (Met 769 and Cys 751). A flexible ligand docking was performed to this grid representation of the receptor binding site followed by scoring the ligand–receptor interaction. The Autodock scores are ranked taking into account the ligand–receptor interaction energy, conformational strain energy of the ligand, conformational entropy loss and desolvation effects. Docking was carried out using Autodock program, an automated and robust docking algorithm based on the Lamarckian genetic algorithm (GA). The software packages Accelrys (INSIGHT-II) and molecular operating environment (MOE) was used to visualize and analyze chemical structures.

To set up a methodology to analyze the docking of TCM compounds to the tyrosine kinase domain of EGFR, an initial docking control study was performed with inhibitor in the crystal structure, erlotinib. A docking operation was carried out in the grid constructed at the binding cavity (dimension of 60 and 120 $Å^3$) to check for the consistency in the results. The *in silico* docking procedure generated the same docking position of erlotinib in EGFR-TK as already known from the published crystal structure of EGFR-TK bound to erlotinib (Protein Data Bank structure PDB 1M17). This control experiment served as confirmation that our docking approach produced valid data. Further, the predicted Ki (pKi) values matched as reported in the literature (Ki = 0.7 ± 0.1 nM). The self-docking of the validated crystal structure of EGFR tyrosine kinase domain (EGFR-TK) (Protein Data Bank 1M17) with erlotinib yielded a docked energy of −13.42 kcal/mol (Fig. 1) [4]. Thus, permissive cut-off docked energy was set to −11 kcal/mol (80% of docked energy in the control self-docking with erlotinib) and the frequency of occurrence of conformations in each cluster was set to at least 10 conformations, in order to select potential candidates during the docking operation. The ligand–protein interaction was analyzed using the LPC tool [18].

2.2. Drugs

Camptothecin and, camptothecin, 20-(N,N-diethyl) glycinate (NSC 364830) were kindly provided by the Drug Synthesis and Chemistry Branch, Chemotherapeutic Agents Repository, National Cancer Institute, USA. Erlotinib was obtained from Target Therapeutics Inc. (Oakland, CA, USA). The chemical structures of the three compounds are shown in Fig. 1.

2.3. Cell lines

The establishment of the parental human glioblastoma cell line, U87MG and its derivatives, which overexpress exogenous wild-type EGFR (U87MG.wtEGFR-2N), tyrosine kinase-deficient EGFR (U87MG.DK-2N), or constitutively active EGFR with a genomic deletion of exons 2–7 (U87MG.ΔEGFR) has been described elsewhere [19]. The cell lines were kindly provided by Dr. W.K. Cavenee (Ludwig Institute for Cancer Research, San Diego, CA, USA). Cell culture conditions of these cell lines were as described [20].

2.4. XTT proliferation assay

The toxicity of compounds was determined by means of the Cell Proliferation Kit II (Roche Diagnostics, Mannheim, Germany). This test is based on the cleavage of the yellow 2,3-bis[2-methoxy-4-nitro-5-sulfophenyl]-*2H*-tetrazolium-5-carboxanilide inner salt (XTT) by ubiquitous dehydrogenases leading to the formation of an orange formazan dye [21]. The amount of dye is commensurate to the number of metabolic active cells. Fresh stock solutions of each compound were prepared in DMSO at a concentration of 100 mM. A dilution series ranging from 10^{-9} to 10^{-3} M was prepared using DMEM medium to perform the XTT test. Cells were diluted to a final concentration of 1×10^5 cells/mL. One hundred micro-liters of the cell suspension were sowed into the wells of a 96-well culture plate (Costar, Corning, USA). Marginal wells were filled with 100 μL of pure medium in order to minimize effects of evaporation. Besides, wells filled with medium were required to determine the background absorbance caused by non-metabolized XTT. A row of wells containing cells was left untreated and another row of wells containing cells was treated with 1 μL DMSO and this served as solvent control. The other rows of wells containing cells

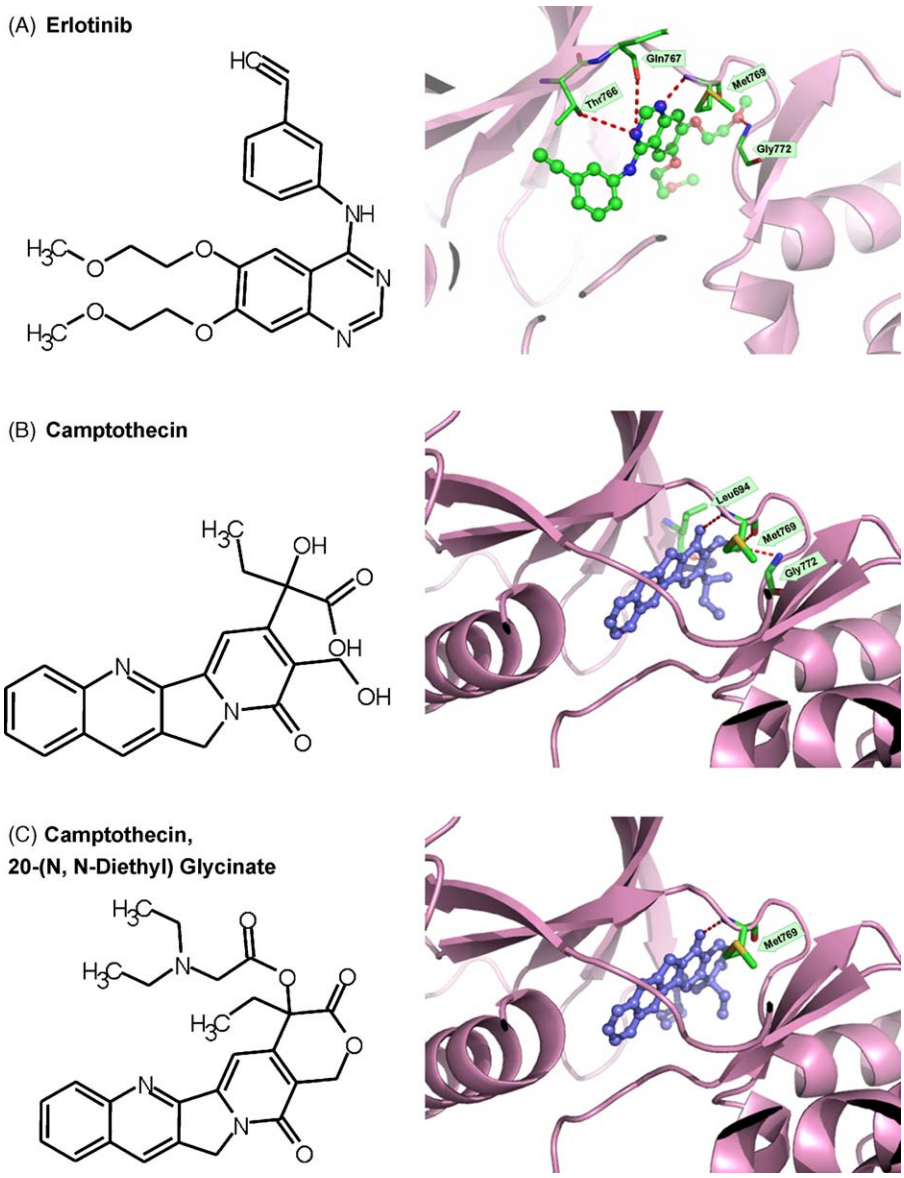

Fig. 1. Chemical structures of putative EGFR inhibitors and molecular docking studies in the EGFR-TK binding pocket. Binding mode of erlotinib (A), CPT (B) and CPTg (C) in ball and stick at the binding pocket of EGFR-TK (*in pink*). The residues involved in hydrogen bond interaction are labeled shown in *green sticks* with the interacting atom in *red dotted lines*. (For interpretation of the references to color in this figure legend, the reader is referred to the web version of the article.)

were supplemented with different concentrations of compound. Each concentration was tested in at least two independent plates containing different batches of cells.

After incubation for 72 h with compounds at 37 °C, 5% CO_2 in humidified atmosphere, XTT reagent was freshly prepared and added to each well as specified by the manufacturer: XTT-labeling reagent and electron-coupling reagent were mixed in a ratio of 50:1 and 50 μL of this mixture were added to each well of the 96-well plate. The plates were incubated for about 3 h at 37 °C, 5% CO_2 in humidified atmosphere and read out after incubation. Quantification of cell cytotoxicity was performed in an ELISA plate reader (Bio-Rad, München, Germany) at 490 nm with a reference wavelength of 655 nm. Absorbance values at both wavelengths were subtracted. The cytotoxic effect of the treatment was determined as percentage of viability and compared to untreated cells [22]. The toxicity of compounds was determined by means of the formula:

$$\text{Cell viability}\,[\%] = \frac{\text{Absorbance of sample cells}}{\text{Absorbance of untreated cells}} \times 100.$$

Simple ligand binding module of Sigma plot software (version 10.0) was used for analysis.

2.5. RNA isolation

Total RNA of transduced and non-transduced U87MG human glioblastoma cells was extracted from the test samples using RNeasy® Mini Kit (Qiagen Inc., Valencia, CA, USA) according to the manufacturer's instructions to obtain highly pure RNA. Isolated total RNA was re-suspended in sample buffer provided by the manufacturer. The concentration and quality of total RNA was verified by electrophoresis using the total RNA Nano-chip assay on an Agilent 2100 Bioanalyzer (Agilent Technologies GmbH, Berlin, Germany). Only samples with RNA index values greater than 8.5 were selected for expression profiling. RNA concentrations were determined using the Nano-Drop spectrophotometer (Nano-Drop Technologies, Wilmington, DE). All of the RNA samples were stored at −80 °C until used for microarray analysis.

2.6. Probe labeling and Illumina Sentrix BeadChip array hybridization

Biotin-labeled cRNA samples for hybridization on Illumina Mouse Sentrix-8 BeadChip arrays (Illumina Inc., San Diego, CA, USA) were prepared according to Illumina's recommended sample labeling procedure based on a previously published protocol [22]. In brief, 250 ng total RNA were used for complementary DNA (cDNA) synthesis, followed by an amplification/labeling step (in vitro transcription) to synthesize biotin-labeled cRNA according to the MessageAmpII aRNA Amplification kit (Ambion, Inc., Austin, TX). Biotin-16-UTP was purchased from Roche Applied Science, Penzberg, Germany. The cRNA was column purified according to TotalPrep RNA Amplification Kit, and eluted in 60 L of water. Quality of cRNA was controlled using the RNA Nano-Chip Assay on an Agilent 2100 Bioanalyzer and spectrophotometrically quantified (Nano-Drop).

Hybridization was performed at 58 °C, in GEX-HCB buffer (Illumina Inc.) at a concentration of 50 ng cRNA/μL, unsealed in a wet chamber for 20 h. Spike-in controls for low, medium and highly abundant RNAs were added, as well as mismatch control and biotinylation control oligonucleotides. Microarrays were washed twice in E1BC buffer (Illumina Inc.) at room temperature for 5 min. After blocking for 5 min in 4 mL of 1% (w/v) Blocker Casein in phosphate buffered saline Hammarsten grade (Pierce Biotechnology, Inc., Rockford, IL), array signals are developed by a 10 min incubation in 2 mL of 1 μg/mL Cy3-streptavidin (Amersham Biosciences, Buckinghamshire, UK) solution and 1% blocking solution. After a final wash in E1BC, the arrays are dried and scanned.

2.7. Scanning and data analysis

Microarray scanning was done using a Beadstation array scanner, setting adjusted to a scaling factor of 1 and PMT settings at 430. Data extraction was done for all beads individually, and outliers are removed when >2.5 MAD (median absolute deviation). All remaining data points are used for the calculation of the mean average signal for a given probe, and standard deviation for each probe was calculated.

Data analysis was done by normalization of the signals using the cubic spline algorithm after background subtraction, and differentially regulated genes are defined by calculating the standard deviation differences of a given probe in a one-by-one comparison of samples or groups. Pathway analysis was done by using the Ingenuity Pathways Analysis software (version 5.5) from Ingenuity Systems (Redwood City, CA, USA).

2.8. Real-time RT-PCR

The experiment was done on the Roche LC480 using ABgene Mastermix "CM 215-A" and Roche Universal Probe Library. Oligos were designed using Roche ProbeFinder Webservice (https://qpcr2.probefinder.com/organism.jsp) and were synthesized by MWG. Two versions were designed per gene. All analyzed variants span an intron to prevent cross-reactions with possible genomic DNA contamination.

Total reaction volume was 10 μL. We used 400 nM final oligo concentration each, 100 nM final probe concentration and 6.3 ng RNA (transcribed in cDNA using Superscript) per reaction. We used transcribed cDNA from RNA obtained from untreated cells or drug-treated cells at the 50% inhibition dose (IC_{50}). No DNAse digest was done. Genes identified by microarray analyses were exemplarily analyzed for validation by means of real-time RT-PCR. The housekeeping genes served as reference as described [22].

All measurements are done in triplicates to calculate mean values and standard deviations. To calculate normalized mRNA expression values, we measured the sample's crossing point (expressed as a cycle number), the efficiency of the reaction, and the number of cycles completed to determine how much the DNA concentration must have increased for each sample by the end of the amplification. The analysis uses these calculations to compare the samples and generate the ratios as indicated by the manufacturer (Roche, Penzberg, Germany). The final ratio resulting from the calibrator normalized relative quantification is a function of PCR efficiency and of the determined crossing points. The "concentration ratio" was determined as the ratio of the target and the reference genes in the specific sample. To calculate the change of expression between untreated (calibrator) and drug-treated samples the concentration ratios of the sample is divided by the concentration ratio of the calibrator. This value is the "normalized ratio".

3. Results

3.1. Docking studies

A total of 410 chemical structures of cytotoxic phytochemicals from our natural product database [18] were individually docked into the defined grid of the validated crystal structure of the EGFR tyrosine kinase domain for conformational search using the Autodock program. Hundred cycles of docking with about 250,000 energy evaluations in each cycle, without any flexibility constraints on the ligand, were carried out, which sampled all possibilities of conformations of the ligand in each cycle to find out the potential candidates that can interact with the tyrosine kinase activity site. Autodock clustering was performed based on the similarities in binding modes and affinities in these cycles. The Autodock clustering output contains information about the cluster size, frequencies of occurrence, mean energies, inhibition constant and root mean square deviations within the cluster.

With the set energy cut-off value of −11 kcal/mol, one of the candidates obtained was camptothecin, 20-(N,N-diethyl) glycinate (NSC 364830). Visual inspections of this compound showed that it bound to the same site as erlotinib (ATP-binding pocket). Then, we also docked camptothecin as lead compound of camptothecin, 20-(N,N-diethyl) glycinate and found that campthotecion also bound to the same domain of EGFR.

Binding site analysis using the LPC tool [18] showed that the orientation of binding of compounds was the same and at least 1 or more binding residues were found to be common in all cases in comparison to erlotinib. Interestingly, the binding of camptothecin and camptothecin 20-N,N-glycinate (further on abbreviated as CPT and CPTg, respectively) differed from the binding of erlotinib. Whereas erlotinib bound to four residues (Thr766, Gln767, Met769, and Gly772), CPT bound to three residues (Leu694, Met769, and Gly772), and CPTg to one (Met769). Met769 binding was a conserved feature for interaction of EGFR with the three compounds. An illustrative view on the binding mode can be seen in Fig. 1.

3.2. Experimental validation

In order to validate the *in silico* molecular docking results, CPT and CPTg were evaluated for their cytotoxic activity towards and downstream signaling mechanisms in EGFR-overexpressing cell lines.

3.3. Cytotoxicity (XTT assays)

Cell viability assays using XTT were performed in transduced and non-transduced U87MG cell lines. CPT and CPTg were tested in a concentration range from 10^{-4} to 10^{-9} M. The dose-response

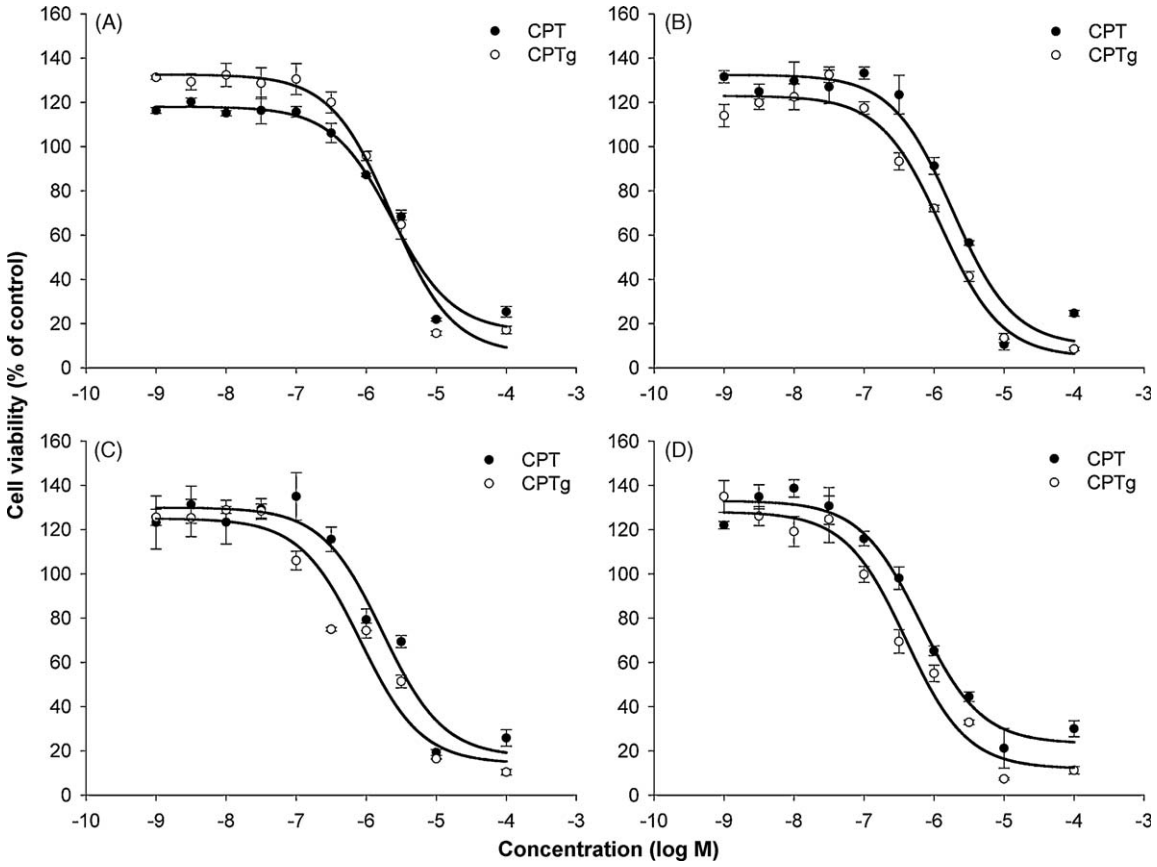

Fig. 2. Dose–response curves for CPTg and CPT in transduced and non-transduced human U87MG glioblastoma cell lines. All values are normalized with the cells treated with 1% DMSO serving a positive control. (A) U87MG, (B) U87MG.ΔEGFR, (C) U87MG.DK-2N and (D) U87MG.wtEGFR-2N.

Table 1
IC_{50} values for camptothecin, 20-(N,N-diethyl) glycinate (CPTg) and camptothecin (CPT) in transduced and non-transduced human U87MG glioblastoma cell lines and respective degrees of sensitization to CPTg or CPT of transduced cell lines in comparison to non-transduced cells. The IC_{50} values were calculated from the dose–response curves shown in Fig. 2.

Cell line	CPTg	Degree of sensitizaton	CPT	Degree of sensitizaton
U87MG	2.39 ± 2.4 μM	–	2.34 ± 6.2 μM	–
U87MG.ΔEGFR	1.82 ± 2.3 μM	1.3	1.28 ± 2.1 μM	1.8
U87MG.DK-2N	1.74 ± 3.1 μM	1.4	0.86 ± 3.3 μM	2.8
U87MG.wtEGFR-2N	0.62 ± 1.9 μM	3.9	0.41 ± 1.2 μM	5.8

*Mean SEM of two independent experiments with each 4-fold determination.
**IC_{50} of the corresponding cell line divided by IC_{50} of U87MG.

curves are shown in Fig. 2, and the IC_{50} values calculated thereof are tabulated in Table 1. CPT displayed a 1.8- to 5.8-fold and CPTg a 1.3- to 3.9-fold increased cytotoxicity in transduced U87MG cell lines in comparison to non-transduced U87MG cells, indicating a preferential activity of these two compounds in EGFR-expressing tumor cells.

Therefore, to further elucidate the molecular pathways involved in exhibiting the cytotoxic effects, a transcriptome-wide microarray approach was performed.

3.4. Microarray analysis

Microarray-based mRNA expression profiling was performed using all four glioblastoma cell lines treated with the two compounds at IC_{50} concentration in duplicates using DMSO-treated cell lines as control. Appropriate quality controls were performed and cut-off values for bead and array standard deviations were derived and set. Individual compound gene expression profiles from respective compound treated cell line were compared and a consensus signature was derived from the intersection.

An overview of the number of up- or down-regulated genes upon treatment of the different U87MG cell lines with CPTg and CPT is given in Fig. 3. The majority of genes regulated by the two compounds were different between the four cell lines. Subsets of genes were commonly regulated in U87MG and U87MG.ΔEGFR, U87MG.DK-2N, and U87MG.wtEGFR-2N cells, respectively. The un-intersected or the uniquely regulated genes for a particular compound were considered as those molecular players that are most relevant for the mechanism of action for such a compound. The variability in the number of such uniquely regulated genes in different EGFR-transduced cell lines suggested the diversity of pathways activated.

Therefore, a pathway profiling was performed on those regulated genes common and unique in U87MG and U87MG.ΔEGFR cells treated with CPTg or CPT. This further gave an insight on those genes that are related to the EGFR-signaling pathway and any other pathway unique for the compounds.

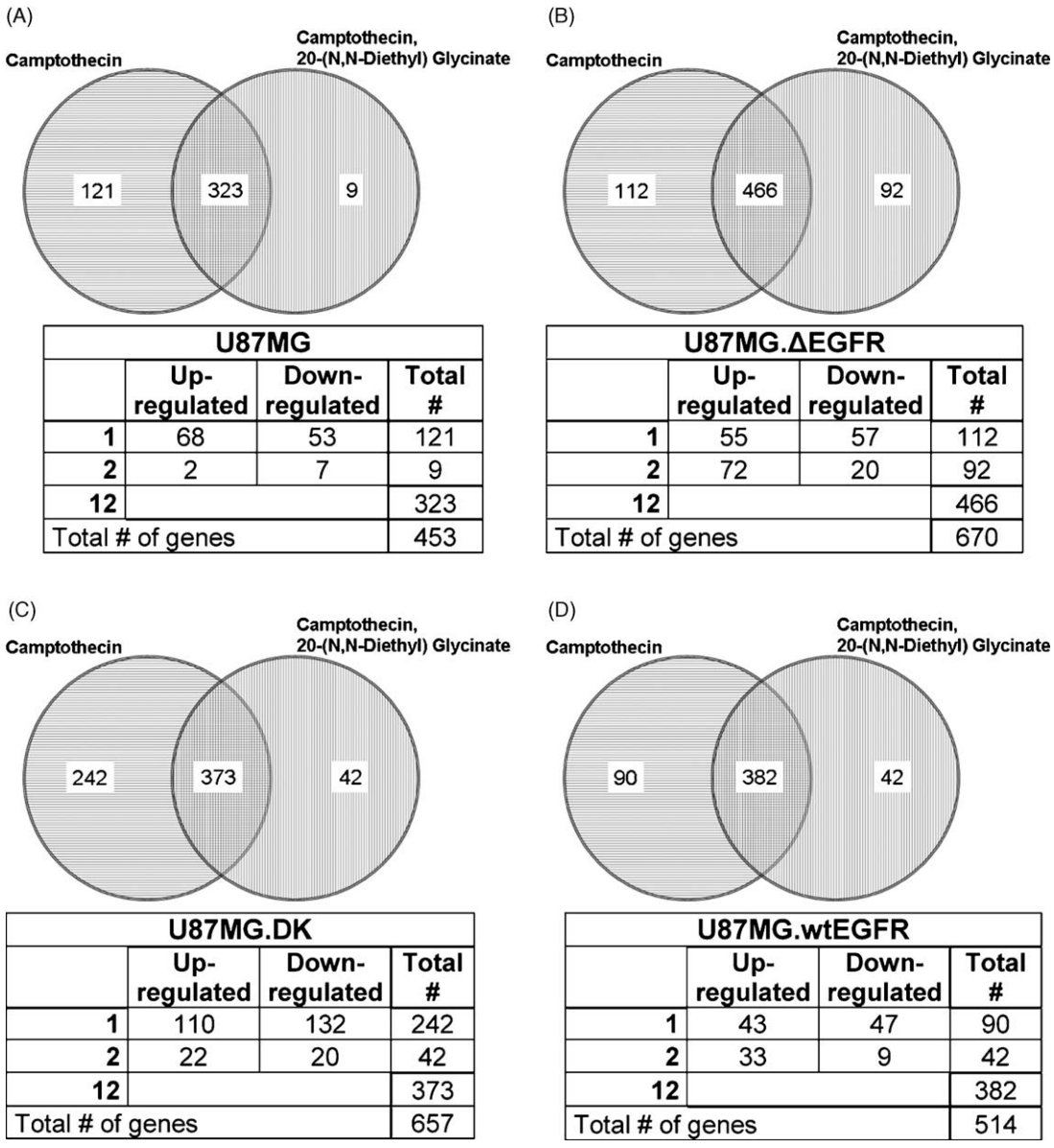

U87MG

	Up-regulated	Down-regulated	Total #
1	68	53	121
2	2	7	9
12			323
Total # of genes			453

U87MG.ΔEGFR

	Up-regulated	Down-regulated	Total #
1	55	57	112
2	72	20	92
12			466
Total # of genes			670

U87MG.DK

	Up-regulated	Down-regulated	Total #
1	110	132	242
2	22	20	42
12			373
Total # of genes			657

U87MG.wtEGFR

	Up-regulated	Down-regulated	Total #
1	43	47	90
2	33	9	42
12			382
Total # of genes			514

Fig. 3. Genes uniquely and commonly regulated in transduced and non-transduced human U87MG glioblastoma cell lines upon treatment with CPT and CPTg. Gene expression profile comparison of cell lines treated with the individual compounds at IC_{50} for 72 h. To discern individual compound responsive genes, gene expression profiles were extracted for each treated cell line and overlaps were examined. The Venn diagram overlaps define the number of genes in common among gene sets. The number of genes contained in each compound's gene expression profile is labeled and tabulated below the Venn diagram. (A) U87MG, (B) U87MG.ΔEGFR, (C) U87MG.DK-2N and (D) U87MG.wtEGFR-2N.

3.5. Pathway profiling of CPTg

By means of Ingenuity Pathway Analysis software, we compared the canonical pathway genes regulated by CPTg in U87MG and U87MG.ΔEGFR cells. As shown in Fig. 4, three out of the top 10 pathways were common and well-above the threshold, −log(*p*-value). The top pathway was G2/M DNA damage checkpoint regulation signaling. The genes involved in this pathway, which were differentially regulated between CPTg-treated and untreated cells, are shown in Fig. 5A for U87MG cells and in Fig. 5B for U87MG.ΔEGFR cells.

Furthermore, we were interested in the differentially regulated genes having a direct or indirect interaction with EGFR signaling. Therefore, we set up a functional pathway analysis independent of canonical pathways, but indicative for EGFR-related signaling. The signaling pathways for U87MG cells (Fig. 6A) and U87MG.ΔEGFR cells (Fig. 6B) constructed by this means further substantiated that the cellular effects of CPTg may indeed be EGFR-mediated.

3.6. Pathway profiling of CPT

In a comparable manner as for CPTg, we profiled the signaling pathways regulated by CPT treatment in U87MG and U87MG.ΔEGFR cells. Interestingly, the G2/M DNA damage checkpoint regulation pathway, which appeared at first place after CPTg treatment (Fig. 5), was now on second place upon CPT treatment (Fig. 7). The aryl hydrocarbon receptor signaling route appeared at first place in U87MG and U87MG.ΔEGFR cells after CPT treatment (Fig. 7). For comparison, this pathway appeared at third place after CPTg treatment (Fig. 5). A considerable number of genes regulated by CPT were related to EGFR signaling in both cell lines (Fig. 8), which compares to the situation observed after CPTg treatment (Fig. 6).

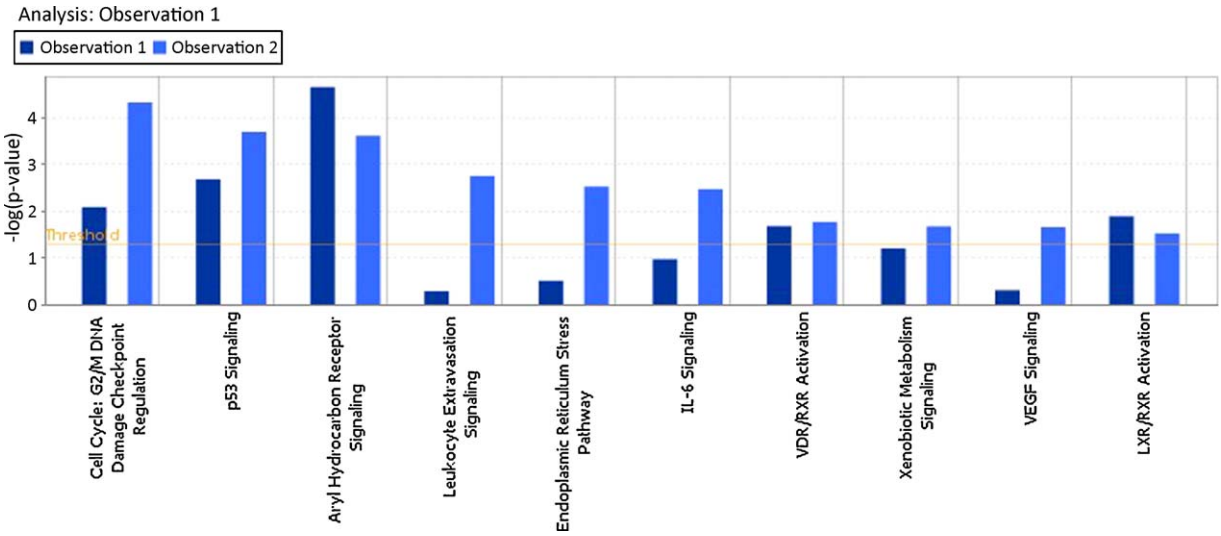

Fig. 4. Canonical pathway analysis for CPTg-treated U87MG and U87MG.ΔEGFR cell lines by the Ingenuity Pathway Analysis software. Each bar represents the ratio of the number of genes that were regulated in a particular canonical pathway. Only the top 10 canonical pathways that were affected by drug treatment are listed and were compared between both cell lines at IC_{50} concentration for 72 h. Observation 1 (*in dark grey*) shows U87MG cells and Observation 2 (*in light grey*) shows U87MG.ΔEGFR cells.

3.7. Real-time RT-PCR

For exemplarily validation of the mRNA expressions obtained by microarray analyses, we performed real-time RT-PCR. Four genes (two up- and two-down-regulated ones upon CPT treatment) were selected and were quantified by RT-PCR (Table 2). The correlation coefficient between mRNA expression values determined by microarray hybridization and real-time RT-PCR was $R = 0.70$, indicating a high degree of concordance between results obtained by microarray hybridization and real-time RT-PCR.

4. Discussion

In the present investigation, we demonstrated by interdisciplinary techniques such as molecular docking and microarray analysis that the cytotoxic effects of camptothecin (CPT) and camptothecin 20-N,N-glycinate (CPTg) were more pronounced in U87MG cell lines transduced with different *EGFR* expression vectors.

It is noteworthy that our three-dimensional modeling approach revealed binding of CPT and CPTg at the same pharmacophore of

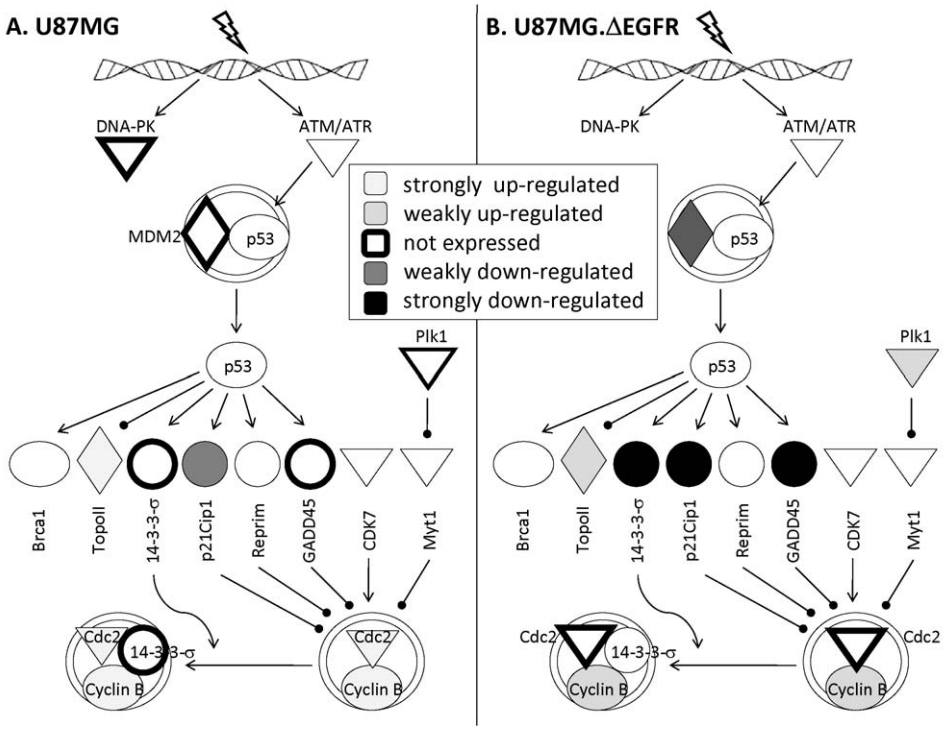

Fig. 5. Genes related to the cell cycle: G2/M DNA damage checkpoint regulation pathway after CPTg treatment in U87MG cells (A) and U87MG.ΔEGFR cells (B). This pathway was identified as the top canonical pathway by the Ingenuity Pathway Analysis software.

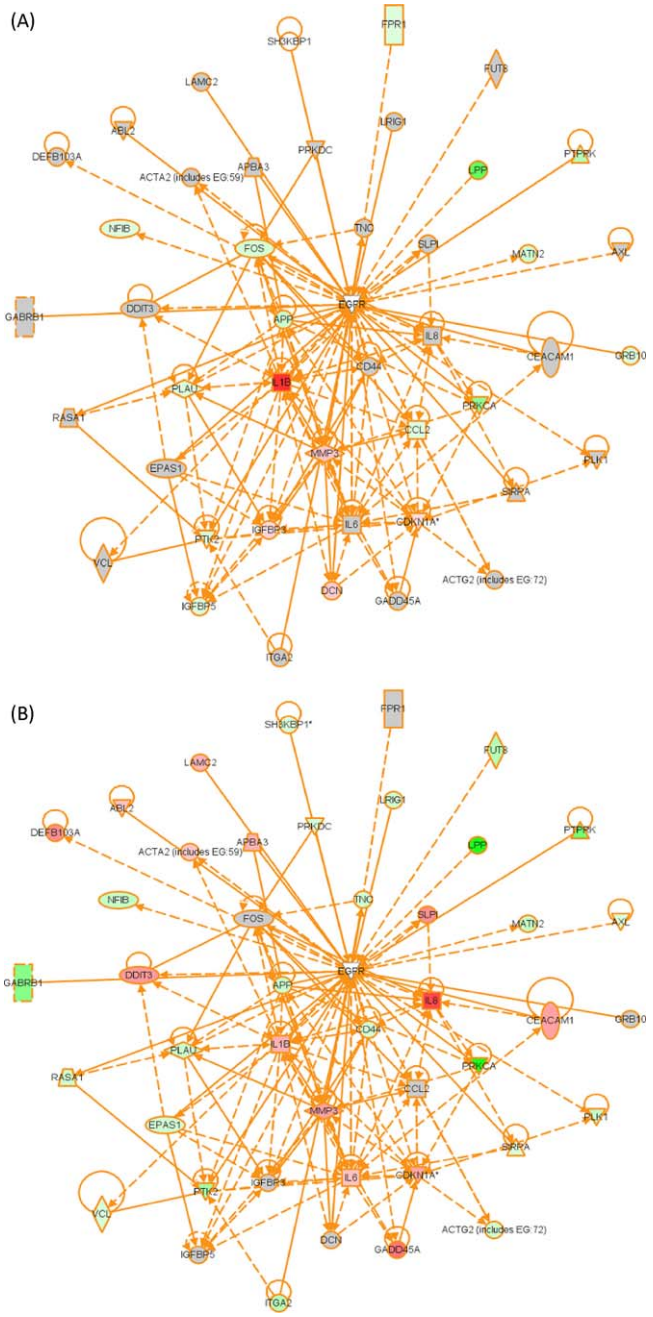

Fig. 6. Genes related to EGFR-signaling pathway that are differentially regulated in both CPTg-treated U87MG (A) and U87MG.ΔEGFR cell lines (B). Pathway analysis was seeded with EGFR (as seen in the centre of the figure), while the other genes were brought into the network by the Ingenuity Pathway Analysis program based on their known relationships to EGFR. *Red color* indicates up-regulation and *green color* indicates down-regulation of transcription while the *grey* blocks indicate genes that are not expressed in that particular cell line in comparison to the other cell line. (For interpretation of the references to color in this figure legend, the reader is referred to the web version of the article.)

EGFR than erlotinib, however, at different amino acids. Erlotinib is a well-established small molecule inhibitor of EGFR, whose activity is already hampered by the development of resistance due to point mutations [23–25]. These point mutations in the tyrosine kinase domain prevent binding of erlotinib rendering tumor cells resistant to EGFR. Our results imply that resistance towards erlotinib may be overcome by CPTg, since it binds to different amino acids in the erlotinib pharmacophore. Thereby, CPTg inhibits phosphate-binding and, hence, signal transduction of EGFR. This point of view is supported by the fact that U87MG.ΔEGFR and U87MG.DK-2N cells are unresponsive to erlotinib (own unpublished results) [26]. U87MG.wtEGFR-2N cells show a weak baseline signaling activity, whereas U87MG.DEGFR cells reveal a strong constitutive signaling. The reason that we found U87MG.DK-2N to be more sensitive to CPT and CPTg might be that the signaling of U87MG.wtEGFR-2N was completely blocked, while the strong signaling of U87MG.ΔEGFR could only partially be inhibited.

Furthermore, we performed transcriptome-wide mRNA microarray experiments to explore the molecular signaling pathways downstream of EGFR, which mediate the cytotoxic actions of these compounds. Microarray and pathway analysis showed similarities and dissimilarities in the regulation of individual gene profiles further supporting the view that individual compounds can activate diverse signaling and metabolic pathways in different cell lines.

The results of the present investigation showed that CPT and CPTg revealed preferential cytotoxicity towards EGFR-overexpressing U87MG cell lines. This is a unique feature, since we previously found that U87MG.ΔEGFR cells exerted resistance but not increased sensitivity towards other natural products such as L-alanosine, homoharringtonine, and artesunate [27–29]. Other groups observed a relationship between EGFR expression and resistance to established drugs [30]. U87MG.ΔEGFR cells have been reported to exert resistance towards cisplatin, paclitaxel, and vincristine [31].

Comparable results have been described in the clinical setting. Tumors overexpressing EGFR are not only more aggressive in their growth behavior, but are also more resistant to combination regimen [32].

Since camptothecins are substrates of BCRP [33–37] and are, hence, part of the spectrum of BCRP-mediated MDR, the preferential sensitivity of EGFR-expressing cells towards camptothecins provide evidence that EGFR-mediated MDR represents a phenotype, which is different from the ABC transporter-type of MDR. Therefore, we were intrigued by the question, which molecular mechanisms downstream of EGFR could contribute to this preferential cytotoxicity of CPT and CPTg.

Therefore, we have performed microarray hybridization experiments. The transcriptome-wide analysis of signaling pathways that are specifically activated in U87.ΔEGFR upon challenge with CPT or CPTg were signaling routes related to aryl hydrocarbon receptor signaling, G2/M damage checkpoint regulation, xenobiotic metabolism signaling and the endoplasmatic reticulum stress pathway.

The aryl hydrocarbon receptor (AhR) signaling pathway is of enormous relevance in carcinogenesis, but also in the conferment of resistance towards chemotherapy. Induction of the *mdr1* gene, which is well-known to induce multidrug resistance, requires the AhR nuclear translocator [38]. Down-regulation of AhR repressor conferred resistance to apoptotic signals [39] and 17-β-estradiol-induced AhR overexpression with the characteristic phenotype of increased proliferation and resistance to apoptosis [40]. Given the general role of AhR for drug resistance, it is worth hypothesizing that AhR may also be involved in response of tumor cells to camptothecins, as indicated by the results of the present investigation.

Xenobiotic metabolism signaling and endoplasmatic reticulum stress pathways are linked to the AhR signaling pathway. Endoplasmatic stress mediates apoptosis [41]. The activation of xenobiotic metabolism signaling and endoplasmatic reticulum stress pathways might indicate the activation of survival mechanisms towards camptothecins either by activation of apoptosis or detoxification mechanisms.

Other signaling routes were also differentially regulated between U87MG.ΔEGFR and parental U87MG cells. Among them

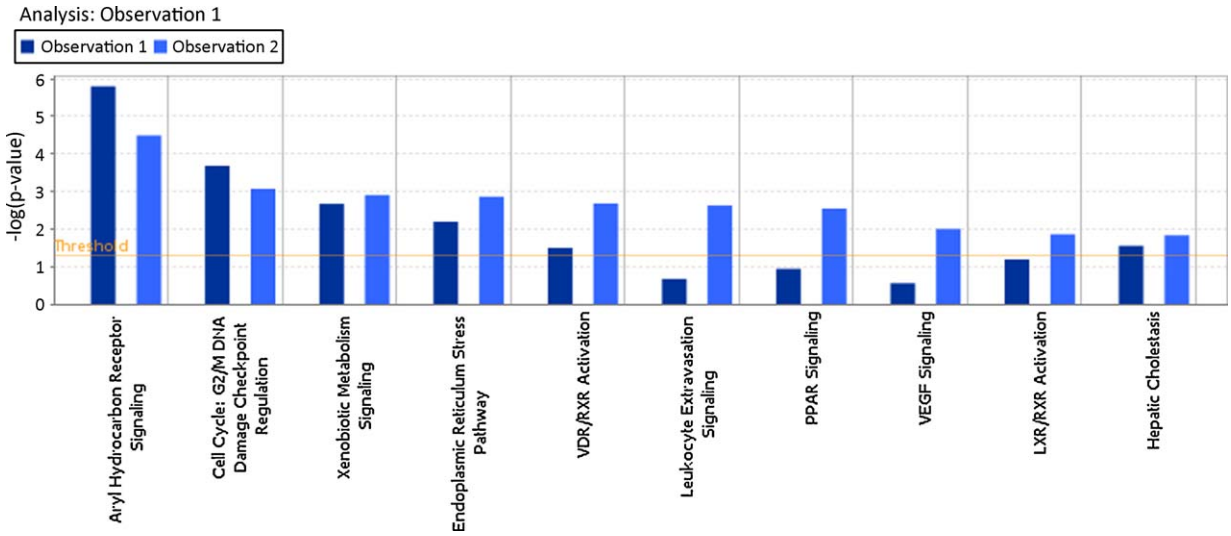

Fig. 7. Canonical pathway analysis for CPT-treated U87MG and U87MG.ΔEGFR cell lines. Details see Fig. 4.

was the signaling route for arrest in the G2/M cell cycle phase. It is well-known that CPT induces G2/M arrest in cancer cells [42]. It comes as no surprise that the signaling route conferring G2/M arrest was activated in our experiments. There is a plethora of investigations pointing to the eminent role of cell cycle arrest for cancer therapy. Cancer cells arresting the cell cycle can resist the detrimental effects of cancer chemotherapy [43,44]. On the other hand, compounds capable to release arrested cells such as caffeine lead to a re-sensitization of cancer cells towards chemotherapy [45]. The fact that camptothecins differentially affects the signaling route for G2/M arrest in U87MG and U87MG.ΔEGFR cells indicates that camptothecins interfere with cell cycle of cancer cells, *e.g.* by DNA topoisomerase I-mediated induction of DNA lesions.

Table 2
Validation of microarray-based mRNA expression by quantitative real-time RT-PCR. Three genes were analysed found to be differently regulated in transduced and non-transduced U87MG glioblastoma cell lines treated or left untreated with CPT.

Cell line	Gene	Method	Untreated cells	CPT-treated cells	Fold change
U87MG	*CDKN1A*	Microarray hybridization	11899.3 ± 279.8*	25647.3 ± 747.7	2,2
		Real-time RT-PCR	0.137 ± 0.0832**	0.428 ± 0.0456	3,1
U87MG	*GADD45A*	Microarray hybridization	982.6 ± 40.1	2071.0 ± 85.0	2,1
		Real-time RT-PCR	1.357 ± 0.5575	3.261 ± 0.1195	2,4
U87MG	*CD44*	Microarray hybridization	10604.6 ± 310.6	5049.6 ± 148.7	−2,1
		Real-time RT-PCR	18.530 ± 7.5930	0.750 ± 0.3049	−24,7
U87MG	*E2F1*	Microarray hybridization	330.0 ± 14.8	110.9 ± 3.7	−3,0
		Real-time RT-PCR	0.003 ± 0.0012	0.001 ± 0.0001	−3,6
U87MG.ΔEGFR	*CDKN1A*	Microarray hybridization	7846.0 ± 197.1	23645.8 ± 595.4	3,0
		Real-time RT-PCR	0.025 ± 0.0013	0.337 ± 0.0139	13,51
U87MG.ΔEGFR	*GADD45A*	Microarray hybridization	513.2 ± 16.6	1889.0 ± 43.6	3,7
		Real-time RT-PCR	0.272 ± 0.0078	1.312 ± 0.0590	4,83
U87MG.ΔEGFR	*CD44*	Microarray hybridization	9454.5 ± 244.6	3587.2 ± 86.6	−2,6
		Real-time RT-PCR	5.653 ± 0.1477	2.916 ± 0.1091	−1,94
U87MG.ΔEGFR	*E2F1*	Microarray hybridization	505.3 ± 18.1	243.0 ± 7.7	−2,1
		Real-time RT-PCR	0.001 ± 0.0001	0.001 ± 0.0001	−1,23
U87MG.DK-2N	*CDKN1A*	Microarray hybridization	5826.0 ± 205.1	26030.5 ± 748.6	4,5
		Real-time RT-PCR	0.018 ± 0.0016	0.605 ± 0.0370	33,41
U87MG.DK-2N	*GADD45A*	Microarray hybridization	644.3 ± 19.7	2100.0 ± 66.2	3,3
		Real-time RT-PCR	0.311 ± 0.0136	2.415 ± 0.1699	7,78
U87MG.DK-2N	*CD44*	Microarray hybridization	8922.9 ± 276.2	4015.8 ± 118.0	−2,2
		Real-time RT-PCR	6.949 ± 0.2229	5.234 ± 0.2903	−1,33
U87MG.DK-2N	*E2F1*	Microarray hybridization	521.4 ± 18.7	195.4 ± 7.3	−2,7
		Real-time RT-PCR	0.001 ± 0.0000	0.001 ± 0.0001	−1,41
U87MG.wtEGFR-2N	*CDKN1A*	Microarray hybridization	6259.6 ± 215.3	25988.7 ± 915.6	4,2
		Real-time RT-PCR	0.024 ± 0.0020	0.618 ± 0.0743	26,1
U87MG.wtEGFR-2N	*GADD45A*	Microarray hybridization	528.3 ± 22.7	6161.4 ± 173.8	11,7
		Real-time RT-PCR	0.362 ± 0.0105	6.715 ± 0.3226	18,5
U87MG.wtEGFR-2N	*CD44*	Microarray hybridization	11109.4 ± 328.4	5449.6 ± 160.8	−2,0
		Real-time RT-PCR	4.843 ± 0.1530	3.621 ± 0.0720	−1,3
U87MG.wtEGFR-2N	*E2F1*	Microarray hybridization	422.7 ± 15.9	609.9 ± 22.1	1,4
		Real-time RT-PCR	0.022 ± 0.0034	0.026 ± 0.0006	1,2

The correlation coefficient between mRNA expression values determined by microarray hybridization and real-time RT-PCR was $R = 0.70$ (Pearson correlation test).
* Average hybridization signal (±SEM).
** Conc. ratio (±Conc. ratio STD).

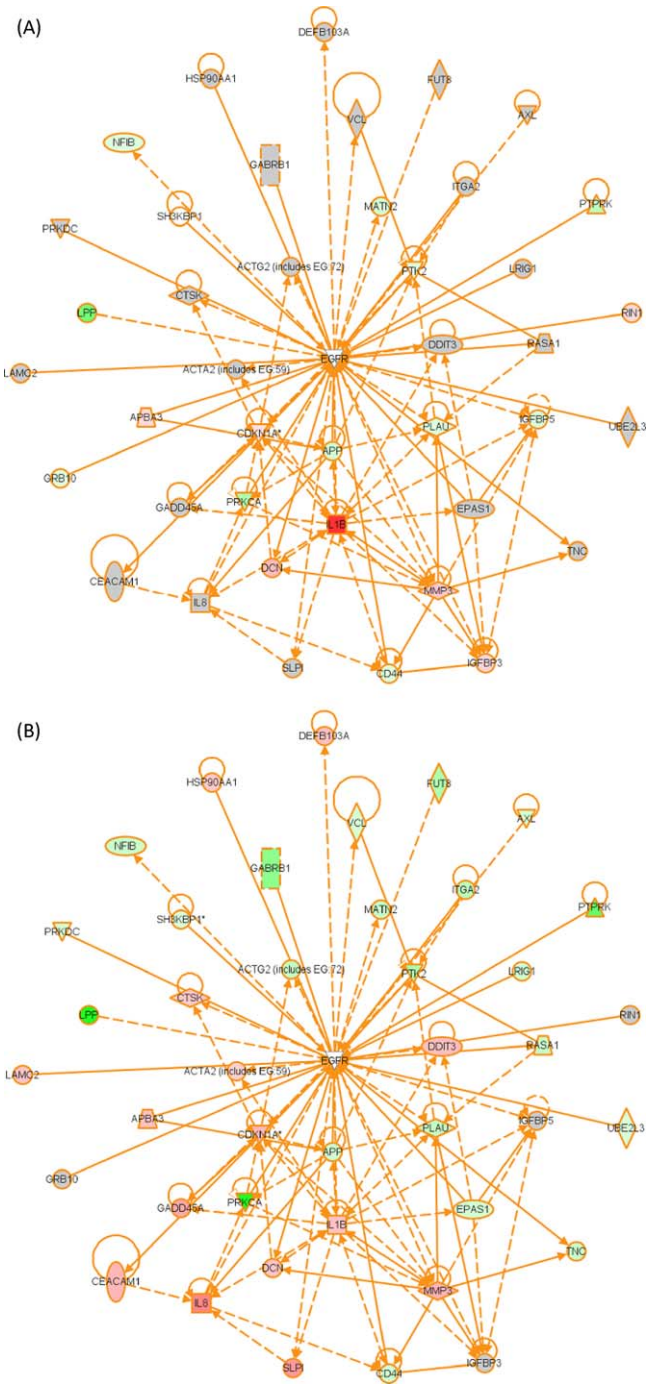

Fig. 8. Genes related to EGFR-signaling pathway that are differentially regulated in both CPT-treated U87MG (A) and U87MG.ΔEGFR cell lines (B). Details see Fig. 6.

In conclusion, we found that both CPT and CPTg preferentially kill EGFR-overexpressing U87MG cell lines. Since EGFR confers drug resistance, CPT and CPTg may be useful for the treatment of otherwise resistant and refractory tumors. Possible explanations for the preferential killing may be binding to EGFR at the tyrosine kinase domain as well as activation of specific EGFR downstream signaling routes.

Acknowledgement

This work has been supported by a grant of the Dietmar Hopp-Foundation (St. Leon-Rot, Germany).

References

[1] Volm M, Efferth T, Mattern J. Oncoprotein (c-myc, c-erbB1, c-erbB2, c-fos) and suppressor gene product (p53) expression in squamous cell carcinomas of the lung. Clinical and biological correlations. Anticancer Res 1992;12:11–20.
[2] Volm M, Kästel M, Mattern J, Efferth T. Expression of resistance factors (P-glycoprotein, glutathione S-transferase-pi, and topoisomerase II) and their interrelationship to proto-oncogene products in renal cell carcinomas. Cancer 1993;71:3981–7.
[3] Fox SB, Smith K, Hollyer J, Greenall M, Hastrich D, Harris AL. The epidermal growth factor receptor as a prognostic marker: results of 370 patients and review of 3009 patients. Breast Cancer Res Treat 1994;29:41–9.
[4] Konkimalla VB, Suhas VL, Chandra NR, Gebhart E, Efferth T. Diagnosis and therapy of oral squamous cell carcinoma. Expert Rev Anticancer Ther 2007;7:317–29.
[5] Konkimalla VB, Suhas VL, Chandra NR, Gebhart E, Efferth T. Diagnosis and therapy of oral squamous cell carcinoma. Expert Rev Anticancer Ther 2007;7:317–29.
[6] Hirsch FR, Varella-Garcia M, Cappuzzo F. Predictive value of EGFR and HER2 overexpression in advanced non-small-cell lung cancer. Oncogene 2009;28(Suppl. 1):S32–7.
[7] Oliveira S, van Bergen en Henegouwen PM, Storm G, Schiffelers RM. Molecular biology of epidermal growth factor receptor inhibition for cancer therapy. Expert Opin Biol Ther 2006;6:605–17.
[8] Astsaturov I, Cohen RB, Harari P. Targeting epidermal growth factor receptor signaling in the treatment of head and neck cancer. Expert Rev Anticancer Ther 2006;6:1179–93.
[9] Perea S, Hidalgo M. Predictors of sensitivity and resistance to epidermal growth factor receptor inhibitors. Clin Lung Cancer 2004;6(Suppl. 1):S30–4.
[10] Teicher BA. Next generation topoisomerase I inhibitors: Rationale and biomarker strategies. Biochem Pharmacol 2008;75:1262–71.
[11] Voigt W, Vanhoefer U, Yin MB, Minderman H, Schmoll HJ, Rustum YM. Evaluation of topoisomerase I catalytic activity as determinant of drug response in human cancer cell lines. Anticancer Res 1997;17:3707–11.
[12] Kancherla RR, Nair JS, Ahmed T, Durrani H, Seiter K, Mannancheril A, et al. Evaluation of topotecan and etoposide for non-Hodgkin lymphoma: correlation of topoisomerase-DNA complex formation with clinical response. Cancer 2001;91:463–71.
[13] Skarlos DV, Bai M, Goussia A, Samantas E, Galani E, Tsavdaridis D, et al. Expression of a molecular marker panel as a prognostic tool in gastric cancer patients treated postoperatively with docetaxel and irinotecan. A study of the Hellenic Cooperative Oncology Group. Anticancer Res 2007;27:2973–83.
[14] Ling YH, Donato NJ, Perez-Soler R. Sensitivity to topoisomerase I inhibitors and cisplatin is associated with epidermal growth factor receptor expression in human cervical squamous carcinoma ME180 sublines. Cancer Chemother Pharmacol 2001;47:473–80.
[15] Vallböhmer D, Iqbal S, Yang DY, Rhodes KE, Zhang W, Gordon M, et al. Molecular determinants of irinotecan efficacy. Int J Cancer 2006;119:2435–42.
[16] Konkimalla VB, Efferth T. Anti-cancer natural product library from traditional Chinese medicine. Comb Chem High Throughput Screen 2008;11:7–15.
[17] Efferth T, Konkimalla VB, Wang YF, Sauerbrey A, Meinhardt S, Zintl F, et al. Prediction of broad spectrum resistance of tumors towards anticancer drugs. Clin Cancer Res 2008;14:2405–12.
[18] Sobolev V, Sorokine A, Prilusky J, Abola EE, Edelman M. Automated analysis of interactomic contacts in proteins. Bioinformatics 1999;15:327–32.
[19] Huang HS, Nagane M, Klingbeil CK, Lin H, Nishikawa R, Ji XD, et al. The enhanced tumorigenic activity of a mutant epidermal growth factor receptor common in human cancers is mediated by threshold levels of constitutive tyrosine phosphorylation and unattenuated signaling. J Biol Chem 1997;272:2927–35.
[20] Nagane M, Coufal F, Lin H, Bögler O, Cavenee WK, Huang HJ. A common mutant epidermal growth factor receptor confers enhanced tumorigenicity on human glioblastoma cells by increasing proliferation and reducing apoptosis. Cancer Res 1996;56:5079–86.
[21] Scudiero DA, Shoemaker RH, Paull KD, Monks A, Tierney S, Nofziger TH, et al. Evaluation of a soluble tetrazolium/formazan assay for cell growth and drug sensitivity using human and other tumor cell lines. Cancer Res 1988;48:4827–33.
[22] Konkimalla VB, Blunder M, Korn B, Soomro SA, Jansen H, Chang W, et al. Effect of artemisinins and other endoperoxides on nitric oxide-related signaling pathway in RAW 264.7 mouse macrophage cells. Nitric Oxide 2008;19: 184–91.
[23] Ahmed SM, Salgia R. Epidermal growth factor receptor mutations and susceptibility to targeted therapy in lung cancer. Respirology 2006;11:687–92.
[24] Kwak EL, Jankowski J, Thayer SP, Lauwers GY, Brannigan BW, Harris PL, et al. Epidermal growth factor receptor kinase domain mutations in esophageal and pancreatic adenocarcinomas. Clin Cancer Res 2006;12(14 Pt 1):4283–7.
[25] Gazdar AF. Activating and resistance mutations of EGFR in non-small-cell lung cancer: role in clinical response to EGFR tyrosine kinase inhibitors. Oncogene 2009;28(Suppl. 1):S24–31.
[26] Wang MY, Lu KV, Zhu S, Dia EQ, Vivanco I, Shackleford GM, et al. Mammalian target of rapamycin inhibition promotes response to epidermal growth factor receptor kinase inhibitors in PTEN-deficient and PTEN-intact glioblastoma cells. Cancer Res 2006;66:7864–9.
[27] Efferth T, Gebhart E, Ross DD, Sauerbrey A. Identification of gene expression profiles predicting tumor cell response to L-alanosine. Biochem Pharmacol 2003;66:613–21.

[28] Efferth T, Sauerbrey A, Halatsch ME, Ross DD, Gebhart E. Molecular modes of action of cephalotaxine and homoharringtonine from the coniferous tree Cephalotaxus hainanensis in human tumor cell lines. Naunyn Schmiedebergs Arch Pharmacol 2003;367:56–67.
[29] Efferth T, Sauerbrey A, Olbrich A, Gebhart E, Rauch P, Weber HO, et al. Molecular modes of action of artesunate in tumor cell lines. Mol Pharmacol 2003;64:382–94.
[30] Wosikowski K, Schuurhuis D, Kops GJ, Saceda M, Bates SE. Altered gene expression in drug-resistant human breast cancer cells. Clin Cancer Res 1997;3:2405–14.
[31] Nagane M, Levitzki A, Gazit A, Cavenee WK, Huang HJ. Drug resistance of human glioblastoma cells conferred by tumor-specific mutant epidermal growth factor receptor through modulation of Bcl-XL and caspase-3 like proteases. Proc Natl Acad Sci USA 1998;95:5724–9.
[32] Chakravarti A, Chakladar A, Delaney MA, Latham DE, Loeffler JS. The epidermal growth factor receptor pathway mediates resistance to sequential administration of radiation and chemotherapy in primary human glioblastoma cells in a RAS-dependent manner. Cancer Res 2002;62:4307–15.
[33] Maliepaard M, van Gastelen MA, de Jong LA, Pluim D, van Waardenburg RC, Ruevekamp-Helmers MC, et al. Overexpression of the BCRP/MXR/ABCP gene in a topotecan-selected ovarian tumor cell line. Cancer Res 1999;59:4559–63.
[34] Kawabata S, Oka M, Shiozawa K, Tsukamoto K, Nakatomi K, Soda H, et al. Breast cancer resistance protein directly confers SN-38 resistance of lung cancer cells. Biochem Biophys Res Commun 2001;280:1216–23.
[35] Schellens JH, Maliepaard M, Scheper RJ, Scheffer GL, Jonker JW, Smit JW, et al. Transport of topoisomerase I inhibitors by the breast cancer resistance protein. Potential clinical implications. Ann N Y Acad Sci 2000;922:188–94.
[36] Rajendra R, Gounder MK, Saleem A, Schellens JH, Ross DD, et al. Differential effects of the breast cancer resistance protein on the cellular accumulation and cytotoxicity of 9-aminocamptothecin and 9-nitrocamptothecin. Cancer Res 2003;63:3228–33.
[37] Nagashima S, Soda H, Oka M, Kitazaki T, Shiozawa K, Nakamura Y, et al. BCRP/ABCG2 levels account for the resistance to topoisomerase I inhibitors and reversal effects by gefitinib in non-small cell lung cancer. Cancer Chemother Pharmacol 2006;58:594–600.
[38] Wong PS, Li W, Vogel CF, Matsumura F. Charcterization of MCF mammary epithelial cells overexpressing the Arylhydrocarbon receptor (AhR). BMC Cancer 2009;9:234.
[39] Zudaire E, Cuesta N, Murty V, Woodson K, Adams L, Gonzalez N, et al. The aryl hydrocarbon receptor repressor is a putative tumor suppressor gene in multiple human cancers. J Clin Invest 2008;118:640–50.
[40] Mathieu MC, Lapierre I, Brault K, Raymond M. Aromatic hydrocartbon receptor (AhR).AhR nuclear translocator- and p53-mediated induction of the murine multidrug resistance mdr1 gene by 3-methylcholanthrene and benzo(a)pyrene in hepatoma cells. J Biol Chem 2001;276:4819–27.
[41] Anether G, Tinhofer I, Senfter M, Greil R. Tetrocarcin-A-induced ER stress mediates apoptosis in B-CLL cells via a Bcl-2-independent pathway. Blood 2003;101:4561–8.
[42] Miettinen S, Ylikomi T. Concomitant exposure of ovarian cancer cells to docetaxel, CPT-11 or SN-38 and adenovirus-mediated p53 gene therapy. Anticancer Drugs 2009;20:589–600.
[43] Efferth T, Fabry U, Osieka R. Apoptosis and resistance to daunorubicin in human leukemic cells. Leukemia 1997;11:1180–6.
[44] Johansson M, Persson JL. Cancer therapy: targeting cell cycle regulators. Anticancer Agents Med Chem 2008;8:723–31.
[45] Efferth T, Fabry U, Glatte P, Osieka R. Expression of apoptosis-related oncoproteins and modulation of apoptosis by caffeine in human leukemic cells. J Cancer Res Clin Oncol 1995;21:648–56.